Carbene derivatives of $[Ir_4(CO)_{12}]$. Crystal structures of $[Ir_4(CO)_{12-x}(\overline{COCH_2CH_2O})_x]$ $(x=1, 2, 3)$

Giacomo Bondietti*, Renzo Ros** and Raymond Roulet†
Institut de Chimie Minérale et Analytique de l'Université, 3 place du Château, CH-1005 Lausanne (Switzerland)
Fabrizio Musso and Giuliana Gervasio
Dipartimento di Chimica Inorganica, Chimica Fisica e Chimica dei Materiali dell' Università, via Giuria 7, I-10125 Turin (Italy)

(Received June 5, 1993)

Abstract

$[Ir_4(CO)_{12}]$ reacts with oxirane in the presence of Br^- to give $[Ir_4(CO)_{12-x}(\overline{COCH_2CH_2O})_x]$ $(x=1, 2, 3)$. The structures of the three products were established by X-ray diffraction studies. All ligands are in terminal positions in $[Ir_4(CO)_{11}(\overline{COCH_2CH_2O})]$. The di- and tri-substituted cluster compounds have 3 edge-bridging COs and dioxycarbene ligands in axial positions. The fluxional behaviour of these Ir_4 clusters, as studied by 2D ^{13}C NMR spectroscopy, is due to CO site exchanges localised on one or on three Ir atoms.

Introduction

Dioxycarbene complexes have been obtained by Angelici and co-workers [1, 2] from reactions of $Fe(CO)_5$, $Mn_2(CO)_{10}$, $Re_2(CO)_{10}$ and $M_3(CO)_{12}$ (M = Fe, Ru, Os) with oxirane. Carbonyl ligands in $Ir_4(CO)_{12}$ have CO stretching force constants higher than *c.* 17 mdyne/Å and should also be susceptible to nucleophilic attack by oxirane. We report here on the synthesis of the first carbene Ir_4 carbonyl clusters, on their fluxional behaviour in solution, and on the crystal structures of $[Ir_4(CO)_{12-x}(\overline{COCH_2CH_2O})_x]$.

Experimental

Syntheses

All reactions were carried out under nitrogen using standard Schlenk techniques. $NEt_4[Ir_4(CO)_{11}Br]$ (**1**) was prepared by the literature method [3]. Microanalyses were carried out by Ilse Beetz Microanalytisches Laboratorium, Kronach, Germany.

*Taken in part from the doctoral dissertation of G.B., EPF Lausanne.

**Permanent address: Istituto di Chimica Industriale dell' Università, via Marzolo 9, I-35131 Padua, Italy.

†Author to whom correspondence should be addressed.

$[Ir_4(CO)_{11}(\overline{COCH_2CH_2O})]$ (2)

Oxirane (70 ml) was condensed at −50 °C into a 100 ml flask containing **1** (850 mg, 0.66 mmol), NaBr (1.1 g, 10.7 mmol) and 2-bromoethanol (5.9 ml, 83.1 mmol). The disparition of **1** was followed for 78 h at 0 °C by IR spectroscopy. The yellow–orange suspension was filtered on celite and washed with cold CH_2Cl_2 (40 ml). The filtrate was stirred vigorously under CO (1 atm.) for 12 h, following by IR the disparition of the bromo-carbene intermediate (which could not be isolated). The solution was evaporated to 10 ml, filtered and chromatographed through a column of silica gel (25×3 cm) using CH_2Cl_2/hexane 1:2 as eluent. The first fraction was crystallised from CH_2Cl_2/heptane giving **2** (570 mg, 75%). Elution of a second band with CH_2Cl_2 gave **3** (81 mg, 10.3%). *Anal.* Calc. for $C_{14}H_4Ir_4O_{13}$ (1149.1): C, 14.63; H, 0.35. Found: C, 14.52, H, 0.48%. IR in nujol: ν(CO) 2092m, 2050vs, br; in THF: 2091s, 2068sh, 2052vs, 2034vs, 2008s, 1846w, 1833w cm^{-1}. ^1H NMR (CD_2Cl_2): δ 4.75 (s) ppm (CH_2). ^{13}C NMR (CD_2Cl_2, 173 K): see text; CH_2 signal (natural abundance): δ 70.5 ppm (t, J(C, H) = 162 Hz).

$[Ir_4(CO_{10}(\overline{COCH_2CH_2O})_2]$ (3)

Oxirane (70 ml) was condensed at −20 °C into a flask containing $[Ir_4(CO)_{12}]$ (185 mg, 0.17 mmol), NaBr (290 mg, 2.82 mmol) and 2-bromoethanol (2.3 ml). The suspension was stirred at 0 °C for 40 h, filtered and washed with CH_2Cl_2 (20 ml). The yellow filtrate was evaporated to dryness at r.t. The residue was dissolved

0020-1693/93/$6.00

in CH_2Cl_2 (70 ml) and chromatographed through a column of silica gel (4×25 cm) using CH_2Cl_2 as eluent. A first fraction gave **2** (14 mg, 7%). The second fraction was crystallised from CH_2Cl_2/heptane giving **3** (160 mg, 80%). *Anal.* Calc. for $C_{16}H_8Ir_4O_{14}$ (1193.10): C, 16.10; H, 0.67. Found: C, 16.20; H, 0.72%. IR (THF): ν(CO) 2063m, 2033s, 2008s, 1969sh, 1875vw, 1829m, 1815m cm^{-1}. ^1H NMR (CD_2Cl_2, 200 K): δ 4.60 ppm (CH_2). ^{13}C NMR (CD_2Cl_2, 193 K): see text; CH_2 signal (natural abundance): δ 72.9 ppm (t, J(C, H) = 160.6 Hz).

$[Ir_4(CO)_9(\overline{COCH_2CH_2O})_3]$ (4)

Oxirane (25 ml) was condensed at −20 °C into a pyrex tube (100 ml) containing $[Ir_4(CO)_{12}]$ (310 mg, 0.27 mmol), NaBr (1.01 g, 0.99 mmol) and 2-bromoethanol (1.5 ml, 21 mmol). The tube was introduced under N_2 in an autoclave which was heated at 40 °C for 4 days. The autoclave was depressurised at 0 °C, and the yellow suspension filtered and washed with CH_2Cl_2 (4×10 ml), water (3×5 ml), and MeOH (2×5 ml). Recrystallisation from CH_3CN gave **4** (249 mg, 75%). Evaporation of the mother liquor gave **3** (19 mg), and traces of **2**. *Anal.* Calc. for $C_{18}H_{12}Ir_4O_{15}$ (1237.2): C, 17.48; H, 0.98. Found: C, 17.67; H, 1.07%. IR (CH_3CN): ν(CO) 2036s, 2014sh, 1992vs, 1970sh, 1867vw, 1807s cm^{-1}. ^1H NMR (CD_3CN, 298 K): δ 4.40 ppm (CH_2); two minor singlets (5%) observed at 4.48 and 4.17 ppm are probably due to isomers. ^{13}C NMR (TMPA, 233 K): see text; additional minor signals appear at 220.5 (2); 219.1; 214.6; 214.5 (1); 196.4; 195.4 (1); 182.4, 181.4 (2); 177.7; 162.0 (1); 160.3 (2) ppm. The 8 resonances with relative intensities in parentheses are probably due to the isomer of **4** with 3 edge-bridging COs, 2 axial and one radial carbene.

Crystal structures of $[Ir_4(CO)_{12-x}(\overline{COCH_2CH_2O})_x]$ (x = 1, 2, 3)

Intensity data were collected on a Siemens P4 diffractometer and all calculations were performed using the SHELXTL PLUS (PC version) program package. A decrease of two standard reflections measured every 50 reflections was accompanied by a decomposition (darkening) of the orange crystals during data collection, thus necessitating a decay correction of the raw intensities. Direct methods were used to find the heavy atom positions. The remaining non-hydrogen atoms were taken from subsequent difference maps. The hydrogen atoms were put in calculated positions, excluding the disordered carbenic moieties, and refined riding on the corresponding carbon atoms with fixed isotropic thermal parameters.

Data collection and refinement

$[Ir_4(CO)_{11}(\overline{COCH_2CH_2O})]$ (2). The crystal data are: monoclinic, $P2_1/c$ space group; a = 9.490(2), b = 9.746(2), c = 23.432(5) Å, β = 98.90(3)°; V = 2141.1(8) Å^3; Z = 4; μ = 24.845 mm^{-1}; crystal size: 0.5×0.3×0.3 mm. Radiation: Mo Kα (λ = 0.71073 Å); 2θ range: 2.0–55.0°; scan type: 2θ–θ; scan range 2.20° in ω; variable scan speed (3.00 to 15.00°/min in ω); empirical absorption correction applied; 7565 reflections collected; 4892 independent reflections (R_{int} = 6.79%); 3350 observed reflections ($F > 5.0\sigma(F)$); weighting scheme: $w^{-1} = \sigma^2(F) + 0.001F^2$; 281 parameters refined; R = 6.34%; R_w = 7.44%. All non-hydrogen atoms were refined anisotropically, using weighted full-matrix least-squares. The atomic fractional coordinates and thermal parameters (U_{eq}) are given in Table 1.

$[Ir_4(CO)_{10}(\overline{COCH_2CH_2O})_2]$ (3). The crystal data are: orthorhombic, *Pbca* space group; a = 12.44(1), b = 18.02(2), c = 25.55(2) Å; V = 5728(9) Å^3; Z = 8; μ = 18.577 mm^{-1}; crystal size: 0.1×0.2×0.1 mm (obtained by slow crystallisation of **3** from THF at

TABLE 1. Atomic coordinates (×10^4) and equivalent isotropic displacement coefficients (Å^2×10^3, defined as one third of the trace of the orthogonalised U_{ij} tensor) of **2**

	x	y	z	U_{eq}
Ir(1)	3368(1)	4154(1)	1020(1)	26(1)
Ir(2)	3743(1)	1645(1)	586(1)	30(1)
Ir(3)	3220(1)	1920(1)	1671(1)	30(1)
Ir(4)	1148(1)	2426(1)	787(1)	29(1)
C(1)	2261(30)	2644(25)	2281(15)	59(11)
C(2)	1950(47)	4065(36)	3060(15)	89(17)
C(3)	1026(50)	2825(46)	3023(17)	97(20)
O(1)	1289(22)	2099(24)	2536(9)	65(8)
O(2)	2837(27)	3708(22)	2639(9)	72(9)
C(11)	2377(24)	5378(24)	1442(10)	33(7)
O(11)	1702(21)	6043(19)	1686(9)	54(7)
C(12)	5283(27)	4644(26)	1375(13)	43(9)
O(12)	6360(24)	4984(27)	1594(12)	87(11)
C(13)	3164(27)	5101(27)	293(14)	49(10)
O(13)	3126(30)	5669(23)	−127(10)	83(11)
C(21)	3498(28)	2165(27)	−207(12)	43(9)
O(21)	3504(33)	2387(33)	−684(10)	100(13)
C(22)	3302(30)	−252(40)	552(15)	65(13)
O(22)	3003(32)	−1387(23)	491(14)	98(13)
C(23)	5744(29)	1585(27)	767(13)	46(9)
O(23)	6941(21)	1500(29)	897(10)	76(10)
C(31)	2735(47)	167(29)	1817(16)	78(15)
O(31)	2416(48)	−1022(23)	1862(14)	145(20)
C(32)	5135(30)	1989(33)	2041(14)	56(11)
O(32)	6278(28)	1961(29)	2259(12)	93(11)
C(41)	−78(28)	3286(35)	1234(13)	54(11)
O(41)	−781(28)	3951(33)	1470(13)	113(14)
C(42)	235(27)	723(33)	786(11)	48(10)
O(42)	−299(23)	−359(21)	785(10)	66(8)
C(43)	537(28)	3118(30)	28(12)	46(9)
O(43)	147(28)	3518(25)	−425(10)	84(10)

TABLE 2. Atomic coordinates ($\times 10^4$) and equivalent isotropic displacement coefficients ($Å^2 \times 10^3$) of **3**. C label corresponds to the solvent molecule

	x	y	z	U_{eq}
Ir(1)	2316(2)	4238(1)	651(1)	45(1)
Ir(2)	3359(2)	5007(1)	1417(1)	42(1)
Ir(3)	2298(2)	3724(1)	1657(1)	41(1)
Ir(4)	1148(2)	4958(1)	1403(1)	47(1)
C(1)	4955(49)	4742(37)	1319(22)	83(19)
C(2)	6573(41)	4183(35)	1451(18)	82(17)
C(3)	6757(44)	4725(33)	1057(18)	85(18)
C(4)	3410(38)	3673(29)	272(17)	55(13)
C(5)	5071(54)	2938(43)	140(21)	21(18)
C(6)	4225(63)	3016(47)	−409(25)	30(19)
O(1)	5351(31)	4168(25)	1530(14)	92(12)
O(2)	5637(38)	5126(27)	1067(16)	118(15)
O(3)	4405(52)	3451(41)	467(22)	61(20)
O(4)	3432(58)	3525(48)	−208(26)	80(24)
C(5′)	4526(85)	2712(65)	−54(42)	87(35)
C(6′)	4781(134)	3462(106)	−460(61)	188(66)
O(3′)	3724(67)	3104(54)	319(31)	137(30)
O(4′)	4100(95)	3822(74)	−109(44)	208(50)
C(11)	1391(38)	4379(30)	100(17)	65(15)
O(11)	914(30)	4428(23)	−293(14)	94(12)
C(12)	3132(40)	5274(30)	622(18)	61(14)
O(12)	3470(26)	5620(22)	302(12)	78(11)
C(13)	1581(35)	3340(28)	977(15)	47(12)
O(13)	1024(31)	2796(25)	859(14)	93(12)
C(23)	3260(28)	4508(21)	2127(11)	18(8)
O(23)	3365(22)	4545(16)	2581(9)	38(7)
C(21)	3671(31)	5959(27)	1633(14)	33(10)
O(21)	3766(30)	6591(25)	1747(14)	95(13)
C(31)	3315(40)	2978(32)	1714(17)	60(14)
O(31)	3963(35)	2495(26)	1755(15)	106(14)
C(32)	1205(49)	3366(38)	2158(22)	92(20)
O(32)	579(31)	3216(21)	2410(13)	82(12)
C(41)	935(34)	5316(25)	2095(14)	40(12)
O(41)	789(30)	5468(22)	2545(13)	85(11)
C(42)	1132(40)	5855(34)	1065(17)	64(14)
O(42)	1102(28)	6339(23)	767(13)	83(11)
C(43)	−193(42)	4413(32)	1224(17)	59(15)
O(43)	−998(36)	4145(29)	1117(15)	111(15)
C	2510(63)	2540(48)	−1248(28)	150
C	1625(68)	3046(55)	−1299(30)	150
C	1603(69)	3416(51)	−1743(30)	150
C	2728(68)	3287(49)	−1992(28)	150
C	3267(65)	2643(50)	−1733(31)	150

−25 °C). Radiation: Mo Kα ($\lambda = 0.71073$ Å); 2θ range: 2.0–50.0°; scan type: 2θ–θ; scan range 1.80° in ω; variable scan speed (3.00 to 15.00°/min in ω); empirical absorption correction applied; 5065 reflections collected; 4543 independent reflections ($R_{int} = 18\%$); 1593 observed reflections ($F > 6.0\sigma(F)$); weighting scheme: $w^{-1} = \sigma^2(F) + 0.0015F^2$; 193 parameters refined; $R = 5.38\%$; $R_w = 6.74\%$. Only the Ir atoms were anisotropically refined using weighted full-matrix least-squares. One carbenic ligand is disordered and the two positions were refined with 0.5 occupancy factors. The atomic fractional coordinates and the thermal parameters (U_{eq}) are given in Table 2. A pentaatomic ring of solvent (probably THF) with high thermal parameters was located in the crystal and included in the refinement as a carbon ring.

$[Ir_4(CO)_9(\overline{COCH_2CH_2O})_3]$ (4). The crystal data are: orthorhombic, $Cmc2_1$ space group; $a = 12.280(3)$, $b = 18.435(6)$, $c = 12.468(3)$ Å; $V = 2835(4)$ Å^3; $Z = 4$; $\mu = 18.776$ mm^{-1}; crystal size: $0.10 \times 0.10 \times 0.08$ mm. Radiation: Mo Kα ($\lambda = 0.71073$ Å); 2θ range: 2.0–50.0°; scan type: 2θ–θ; scan range 1.80° in ω; variable scan speed (4.00 to 15.00°/min in ω); empirical absorption correction applied; 3912 reflections collected; 2246 independent reflections ($R_{int} = 2.97\%$); 1881 observed reflections ($F > 4.0\sigma(F)$); weighting scheme: $w^{-1} = \sigma^2(F) + 0.0056F^2$; 180 parameters refined; $R = 5.32\%$; $R_w = 7.02\%$. All atoms were anisotropically refined with the exclusion of the atoms belonging to a disordered carbenic moiety. A 0.5 or 0.25 occupancy factor was applied to the two positions of the disordered carbene ligand lying on the crystallographic mirror plane. The atomic fractional coordinates and thermal parameters (U_{eq}) are given in Table 3.

NMR measurements

^{13}C NMR spectra: Brucker WH 360 (90.55 MHz); δ in ppm relative to TMS, J(C, C) in Hz, samples

TABLE 3. Atomic coordinates ($\times 10^4$) and equivalent isotropic displacement coefficients ($Å^2 \times 10^3$) of **4**

	x	y	z	U_{eq}
Ir(1)	1104(1)	1485(1)	5995(1)	31(1)
Ir(2)	0	2433(1)	4720(1)	30(1)
Ir(3)	0	2617(1)	6904(1)	36(1)
C(11)	2236(19)	1454(13)	6917(24)	43(7)
O(11)	2954(25)	1418(16)	7582(21)	82(11)
C(12)	1672(16)	2308(10)	4978(14)	27(5)
O(12)	2512(14)	2568(14)	4681(20)	55(7)
C(13)	0	849(18)	6853(28)	37(8)
O(13)	0	330(14)	7431(21)	61(10)
C(21)	0	3375(16)	4207(23)	38(9)
O(21)	0	3962(15)	3982(30)	66(11)
C(31)	0	2172(19)	8227(28)	38(9)
O(31)	0	1905(17)	9074(25)	59(10)
C(32)	1251(26)	3218(18)	6919(30)	60(9)
O(32)	1937(26)	3627(14)	6895(31)	97(12)
C(1)	1601(17)	689(10)	5073(17)	32(5)
C(2)	1987(28)	−457(14)	4363(22)	56(9)
C(3)	2404(23)	71(13)	3635(21)	51(8)
O(1)	1436(29)	−8(12)	5271(19)	89(9)
O(2)	2085(24)	768(11)	4154(19)	75(8)
C(4)	0	1997(16)	3289(29)	35(6)
C(5)	0	1331(45)	1860(76)	51(17)
C(6)	0	1970(91)	1357(128)	104(44)
O(3)	0	1408(38)	2941(71)	75(20)
O(4)	0	2427(24)	2335(46)	38(10)
O(3′)	704(43)	2057(29)	2595(44)	76(13)
C(5′)	629(48)	1506(28)	1717(51)	49(12)

enriched to *c.* 30% ^{13}CO. 2D ^{13}C NMR spectra: COSY experiments, typically 256t_1 increments with 2-K transients, spectral width 4504 (Fig. 1), 6250 Hz (Fig. 3) in the F_2 domain, and 2252 (Fig. 1), 3125 Hz (Fig. 3) in the F_1 domain; NOESY experiments (mixing times indicated in the text), typically 512 increments with 2-K transients, spectral width 1901.0 (Fig. 1), 6173 (Fig. 3), 6410 (Fig. 4), in the F_2 domain, and 905.5 (Fig. 1), 3086.5 (Fig. 3), 3205 (Fig. 4) in the F_1 domain; a square sine bell was applied in both domains prior to Fourier transformation.

Results and discussion

The reaction of $[Ir(CO)_{11}Br]^-$ (**1**) with excess ethylene oxide in the presence of NaBr and 2-bromoethanol at 0 °C, followed by saturation with CO (1 atm.) and chromatography, gave $[Ir_4(CO)_{11}(\overline{COCH_2CH_2O})]$ (**2**) in good yields and $[Ir_4(CO)_{10}(\overline{COCH_2CH_2O})_2]$ (**3**) as minor product. The same reaction starting with $[Ir_4(CO)_{12}]$ gave **3** in 80% yields and **2** as minor product. Further substitution was achieved by performing the reaction in an autoclave at 40 °C giving $[Ir_4(CO)_9(\overline{COCH_2CH_2O})_3]$ (**4**) (75%).

The solid state structure of **2** has all terminal ligands, as shown by X-ray analysis (see below). The ^{13}C NMR spectrum of **2** enriched in ^{13}CO (*c.* 30%) in CD_2Cl_2 is blocked at 173 K and presents two sets of signals. A first set of 5 signals of relative intensities 1:2:2:4:3 at δ 194.2 (COO), 161.6 (1), 157.8 (2), 156.3 (3+4) and 155.4 (5+6) ppm are observed in the terminal CO region and are due to the unbridged isomer **2u** (Scheme 1). The signal of relative intensity one is assigned to the unique COO group of the carbene ligand. Inspection of a COSY ^{13}C NMR spectrum (Fig. 1(a)), where the only COs which couple significantly are in relative pseudo-*trans* positions, allows the 24 virtually possible assignments to be reduced to only eight which are consistent with the couplings (COO,6), (1,5) and (2,4)(^3J(CO, CO) = 11 ± 1 Hz). One of these is represented in Scheme 1 with the COs labelled 1 to 6 in order of decreasing chemical shift. A second, minor set of 8 signals of relative intensities 2:1:1:1:2:2:1:2 are observed at δ 204.7 (a), 198.1 (b), 191.5 (COO), 174.6 (f), 171.0 (d), 158.4 (c or g), 154.2 (e) and 153.3 (g or c) ppm. Their assignment follows the general observation that in the ^{13}C and ^{31}P NMR spectra of Ir_4 cluster compounds, the δs of the ligands decrease in the positional sequence bridging > radial > axial ≈ apical [4]. The first two signals are clearly due to three edge-bridging COs. The presence of two resonances in the region of radial COs (relative intensities 1:2) implies that the carbene ligand is in axial position with respect to the basal $Ir_3(\mu_2\text{-}CO)_3$ plane. Thus, the

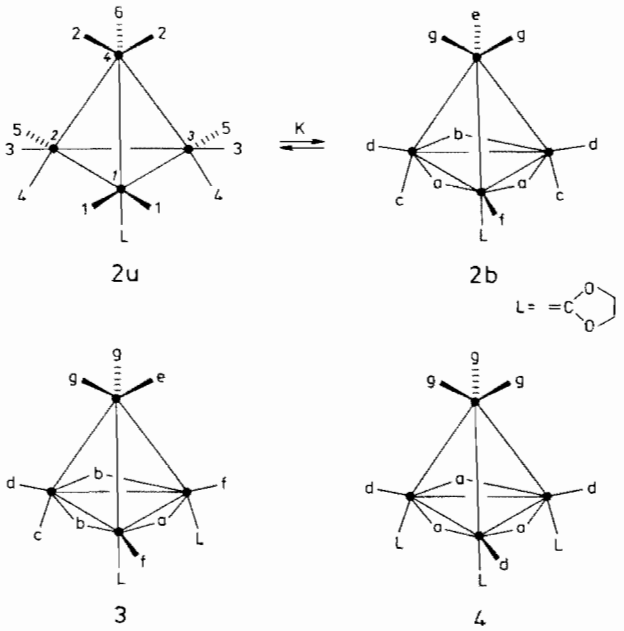

Scheme 1.

second set of resonances corresponds to the bridged isomer **2b** (Scheme 1). Upon gradually raising the temperature to 193 K, the ratio K = [**2u**]/[**2b**] increases from 6.15 to 11.35. The formation of **2u** is thus endothermic. The thermodynamic parameters of the isomerisation equilibrium **2b** = **2u** were calculated from a graph ln K versus $1/T$ giving $\Delta H = 10.8 \pm 0.4$ kJ mol^{-1} and $\Delta S = 8 \pm 4$ J mol^{-1} K^{-1}.

Both isomers are fluxional and the dynamic connectivities of **2u** were deduced from a NOESY ^{13}C NMR spectrum at 188 K (Fig. 1(b), region of terminal COs). A connectivity 1 ↔ 3 ↔ 5 (the exchange 1 ↔ 5 is of second order) is observed at and below 188 K and corresponds to the exchange matrix of a first merry-go-round of 6 COs around either the Ir(1)–Ir(2)–Ir(3) face (for 4 of the 8 possible arrangements) or the Ir(2)–Ir(3)–Ir(4) face (for the remaining ones). A second connectivity 2 ↔ (3 and/or 4) is observed at or above 188 K. A swapping of terminal COs residing on adjacent metal atoms is not possible in a single step. Likewise, a merry-go-round of COs has never been observed when the ground state of the Ir_4 cluster contains a face bearing a radial L, three edge-bridging, and two terminal COs [5]. Therefore, we propose that the connectivity is 2 ↔ 3 ↔ 4, which corresponds to a second merry-go-round taking place on the Ir(2)–Ir(3)–Ir(4) face and which keeps the pseudo-*trans* relationship between L and carbonyl 6. The eight possible assignments are in agreement with the two merry-go-round mechanisms.

At 263 K, two resonances are observed at 157.5 and 155.4 ppm with relative intensities 10:1, respectively (Fig. 2). This is in agreement with the averaging of 10

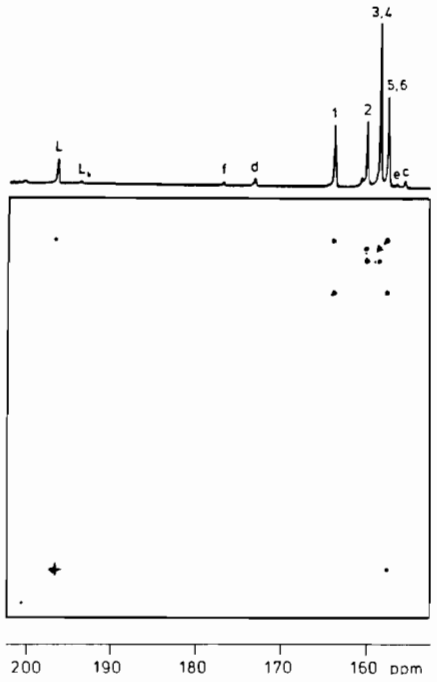

(a)

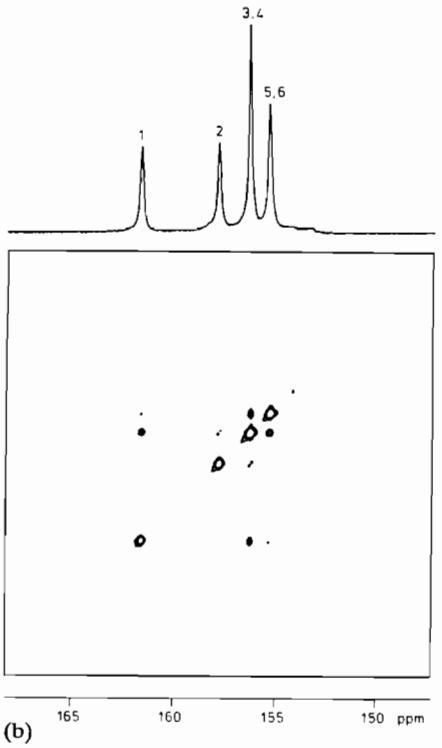

(b)

Fig. 1. (a) COSY ^{13}C NMR spectrum of **2** in CD_2Cl_2 at 173 K. (b) NOESY ^{13}C NMR spectrum of **2u** in CD_2Cl_2 at 188 K (region of terminal COs; mixing time 100 ms).

COs through merry-go-rounds and carbonyl 6 remaining unaffected by these μ_1-CO ↔ μ_2-CO exchanges. Above *c.* 260 K, a third process involving carbonyl 6 in a 3 COs exchange around one metal centre is taking place,

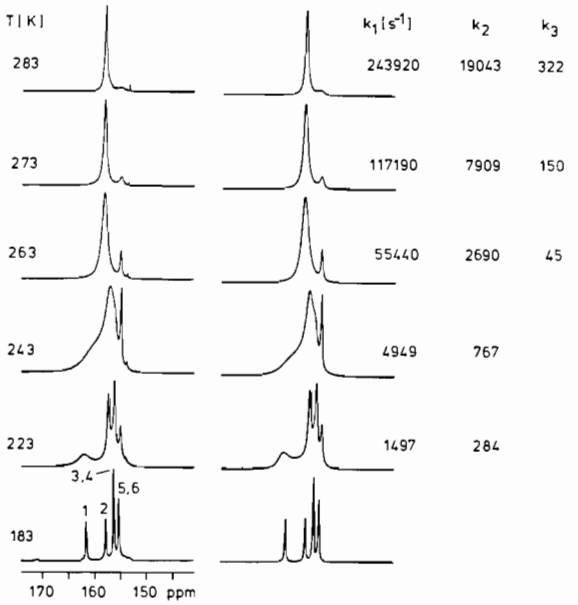

Fig. 2. Experimental and calculated VT ^{13}C NMR spectra of **2** in CD_2Cl_2.

as already observed in other $[Ir_4(CO)_{11}L]$ complexes [5, 6].

Line-shape analysis [7] of the variable-temperature ^{13}C NMR spectra (Fig. 2) was carried out using the following Kubo-Sack matrix elements: $(1,1)=(5,5)=-k_1/2$, $(1,3)=(3,1)=(3,5)=(5,3)=k_1/2$, $(2,3)=(3,2)=(3,4)=(4,3)=k_2/2$, $(4,4)=-k_2/2$, $(2,2)=-k_2/2-k_3$, $(3,3)=-k_1-k_2$, $(6,2)=k_3$, $(2,6)=k_3/2$, $(6,6)=-k_3$, with k_1, k_2, k_3 = rate constants in s^{-1} of the first and the second merry-go-round and of the rotation of 3 COs at one metal centre, respectively. The free enthalpies of activation of these three processes, were calculated from the graph $\ln(k/T)$ versus $1/T$: $\Delta G^{\neq}_{298}=42.3\pm1.0$, 48.7 ± 1.5, and 55.2 ± 0.6 kJ mol^{-1}, respectively. The rotation of apical COs at one metal centre is also the higher activation energy process in other $[Ir_4(CO)_{11}L]$ and $[Ir_4(CO)_9L_3]$ systems [5, 6].

A more general picture of the fluxional behaviour of $[Ir_4(CO)_{11}L]$ clusters arises from the comparison of the ^{13}C NMR studies on **1** [8], **2**, $[Ir_4(CO)_{11}(PR_3)]$ [5, 9, 10] and $[Ir_4(CO)_{11}(t\text{-BuNC})]$ [6, 11]. When the L ligand has a carbon donor atom, the ground state geometry has all terminal ligands. The isomer with three edge-bridging ligands and L in axial position may not be observed, but is in all cases an intermediate in merry-go-round processes. When L has a P or halogen donor atom, the ground state geometry is usually $[Ir_4(CO)_8(\mu_2\text{-}CO)_3L]$. When the edge-bridging COs are asymmetrical, as in **1** [8], the merry-go-round process around the basal face (as well as subsequent changes of basal face) does not pass through an intermediate with all terminal ligands.

The IR spectra of a solution of **3** in THF or of its suspension in nujol have strong absorptions below 1900 cm^{-1} which indicate the presence of bridging COs. Its ^1H NMR spectrum in CD_2Cl_2 at 200 K presents a single resonance for the methylene groups. Therefore, the two carbene ligands occupy equivalent positions on two Ir atoms. The ^{13}C NMR spectrum of a sample enriched in ^{13}CO (*c.* 30%) is blocked at 193 K and presents 8 resonances of relative intensities 1:2:2:2:1:1:2:1 at δ 215.6 (t, J(C, C) = 11.2 Hz), a; 208.9 (t, J(C, C) = 11.2 Hz), b; 195.2, COO; 180.0, f; 174.4, d; 164.2, e; 160.5, g; 156.9, c (Scheme 1 and Fig. 3(a)). The presence of two resonances (3 COs) in the region of radial carbonyls indicates that the two carbene ligands are located on an axial position on two Ir atoms of the basal face, as in the solid state structure (see below). The assignment of carbonyls e and c which are in relative pseudo-*trans* positions is ambiguous and this will have to be taken into account in the discussion.

A 2D NOESY spectrum of **3** in (D8)THF at 213 K shows the dynamic connectivities a ↔ f ↔ b ↔ d (Fig. 3(b)). Therefore, the site exchange process of lowest activation energy is the merry-go-round around the basal face. Linc shapc analysis of the variable temperature ^{13}C NMR spectra using the corresponding exchange matrix gave an free enthalpy of activation of 40.5 ± 0.8 kJ mol^{-1} at 298 K. A second 2D NOESY spectrum taken at 243 K (mixing time: 100 ms) showed a single dynamic connectivity (e or c) ↔ g. Since carbonyl c cannot exchange with g without incorporating other carbonyls in the process, the signal at 164.2 ppm can confidently be assigned to carbonyl e. Coalescence of the signals at 164.2 and 160.5 ppm takes place at *c.* 263 K. Therefore, the second fluxional process is the rotation of the three apical COs about a local C_3 axis. Above 263 K, a third, unidentified process takes place, incorporating carbonyl c in the site exchange, but maintaining the relative pseudo-*trans* positions of carbonyl g and the carbene ligand.

The site exchange processes of lowest activation energy in **2** are the same as in $[Ir_4(CO)_{10}(dppm)]$ (dppm = bis(diphenylphosphino)methane) and $[Ir_4(CO)_{10}(dppa)]$ (dppa = bis(diphenylarsino)methane), but differ from those in $[Ir_4(CO)_{10}(PMePh_2)_2]$ which has a different ground state geometry with three edge-bridging COs, an axial and a radial tertiary phosphine [5, 11]. Therefore, one may conclude that the dynamic behaviour of disubstituted Ir_4 carbonyl clusters with two monodentate L ligands or with one bidentate L-L ligand are identical, as long as the ground state geometry is the same (with two axially located P-, As- or C-donor atoms).

Carbonyl cluster **4** is only sparingly soluble in organochlorinated solvents, but can be studied in CH_3CN, DMSO or TMPA. Its IR spectrum in CH_3CN has two absorptions below 1900 cm^{-1} indicating the presence of bridging COs. The ^{13}C NMR spectrum of a sample enriched in ^{13}CO (*c.* 30%) in TMPA is blocked at 233

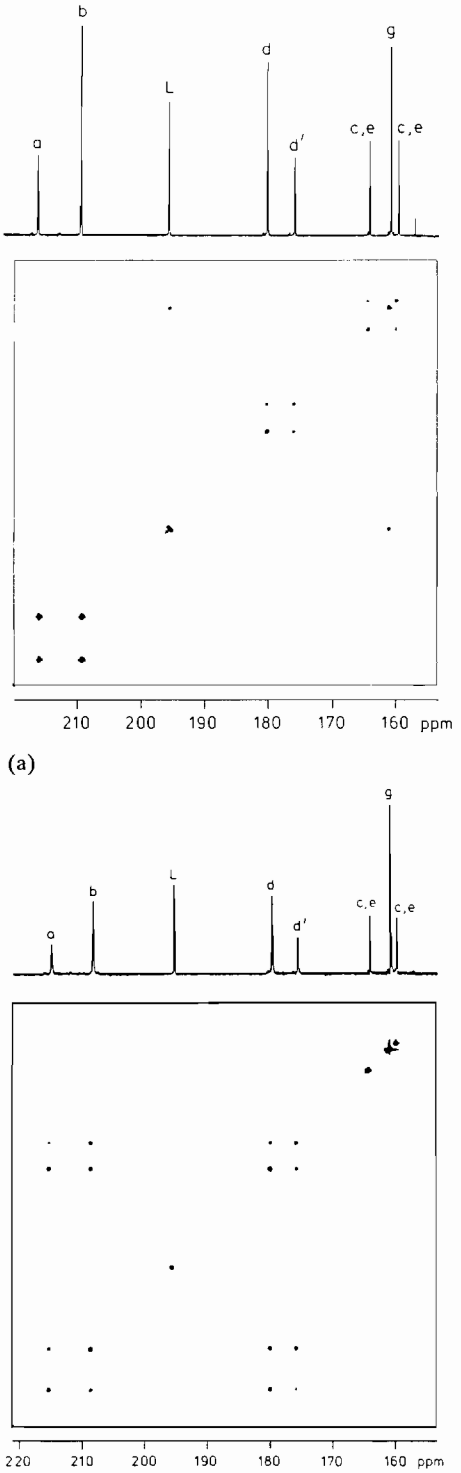

Fig. 3. (a) COSY ^{13}C NMR spectrum of **3** in (D8)THF at 193 K. (b) NOESY ^{13}C NMR spectrum of **3** in (D8)THF at 213 K (mixing time 80 ms).

K and reveals the presence of one major isomer (98%) with four resonances of equal relative intensities at δ 219.2, a; 196.8, COO; 180.7, d; 163.1 ppm, g (Scheme 1). The resonance at 196.8 ppm can confidently be attributed to the equivalent COO groups of the carbene ligands. The presence of one signal in the region of bridging carbonyls and one in that of radial carbonyls indicates that the major isomer of **4** has a ground state geometry with three bridging COs and three axially located, carbene ligands (C_{3v} symmetry), as in the solid state structure (see Fig. 7). One of the minor isomers (<2%) has probably three bridging COs, two axial and one radial carbene ligands ('Experimental'). Fortunately, the presence of the minor isomers does not complicate the dynamic situation. A 2D NOESY spectrum of **4** in TMPA at 263 K (Fig. 4) shows a single dynamic connectivity a↔d. This corresponds to the merry-go-round of the three bridging and the three radial COs around the basal face. The dynamic behaviour of **4** is therefore comparable to that of a trisubstituted Ir_4 carbonyl cluster with a tridentate ligand such as 1,3,5-trithiane [12]. Here again, the absence of linkage between the donor atoms of the non-CO ligands does not introduce additional pathways for the carbonyl site exchanges.

Crystal structures of $[Ir_4(CO)_{12-x}(\overline{COCH_2CH_2O})_x]$ *(x=1, 2, 3)*

Molecular structure of $[Ir_4(CO)_{11}(\overline{COCH_2CH_2O})]$ *(2)*

A perspective view of **2** is shown in Fig. 5, which should also correspond to the geometry of the unbridged

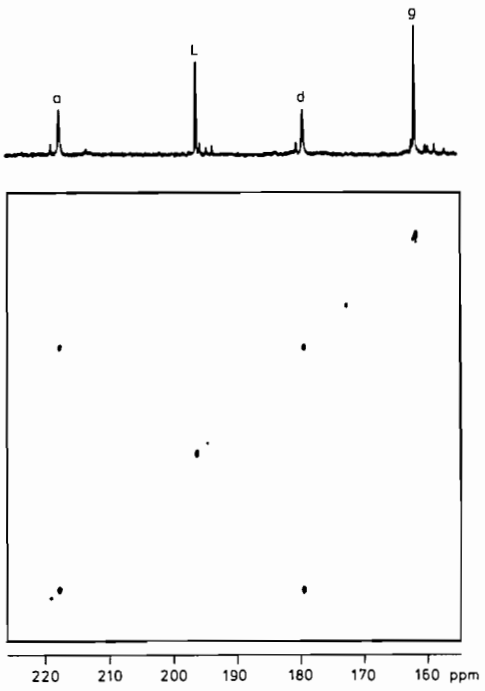

Fig. 4. NOESY ^{13}C NMR spectrum of **4** in TMPA at 253 K (mixing time 100 ms).

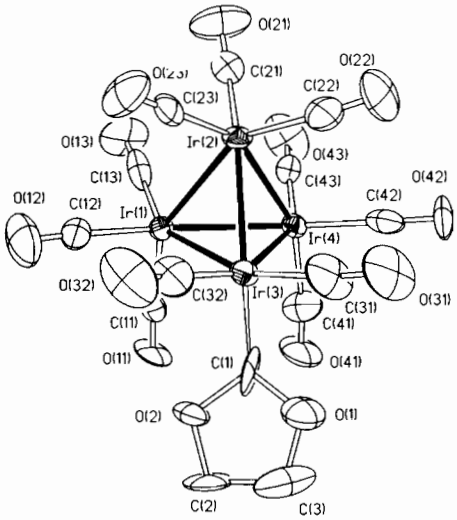

Fig. 5. ORTEP plot (50% of probability) of $[Ir_4(CO)_{11}(\overline{COCH_2CH_2O})]$ (**2**) with atom labelling scheme.

isomer **2u** in solution (C_s symmetry). The molecule can be described as deriving from $[Ir_4(CO)_{12}]$ with one CO group substituted by a carbenic unit $C_3H_4O_2$. The C(1) atom replaces exactly the C atom of a terminal CO group with the same geometry with respect to the cluster (same values of the Ir–Ir–C(1) angles and of the Ir–C(1) distance). The tilting angles of the equatorial COs with respect to the related Ir(1)–Ir(3)–Ir(4) basal plane have values of 12 and 14° around Ir(3), of 11 and 16° around Ir(4) and of 8 and 18° around Ir(1); the axial COs and the Ir(3)–C(1) bond form angles of 82, 82 and 78° with respect to the same previous plane. These values suggest therefore a negligible steric influence of the carbenic ligand. The three Ir–Ir(3) distances are somewhat shorter (mean 2.675(1) Å) than the three other Ir–Ir distances (mean 2.690(1) Å) which are comparable to those of other Ir_4 clusters with unbridged carbonyls [13, 14]. Examination of all Ir–Ir–CO angles does not show any deviation towards an asymmetrical, semi-bridging coordination of COs.

Molecular structure of $[Ir_4(CO)_{10}(\overline{COCH_2CH_2O})_2]$ *(3)*

Figure 6 shows a perspective view of the molecule. Three edges of a triangular face of the Ir_4 tetrahedron are bridged by three carbonyls defining the basal face. The high e.s.d.s due to the poor quality of the crystal do not allow any distinction between symmetrical and asymmetrical bridges. The two carbenic ligands are axial with respect to the basal plane (mean deviation from the plane 0.05 Å). The Ir(3)–C(31), Ir(2)–C(1) and Ir(1)–C(4) bonds form angles of 69, 72 and 70°, respectively, with the Ir(1)–Ir(2)–Ir(3) plane, which are quite different from the corresponding values of **2**. The tilting angles of CO(32), CO(11) and CO(21) groups

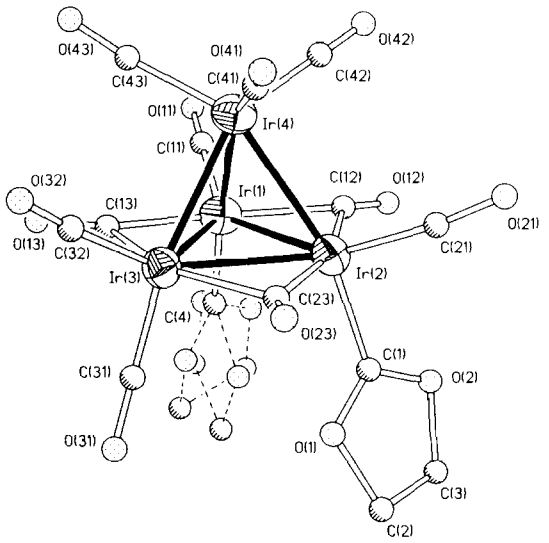

Fig. 6. ORTEP plot (50% of probability) of $[Ir_4(CO)_{10}(\overline{COCH_2CH_2O})_2]$ (**3**) with atom labelling scheme.

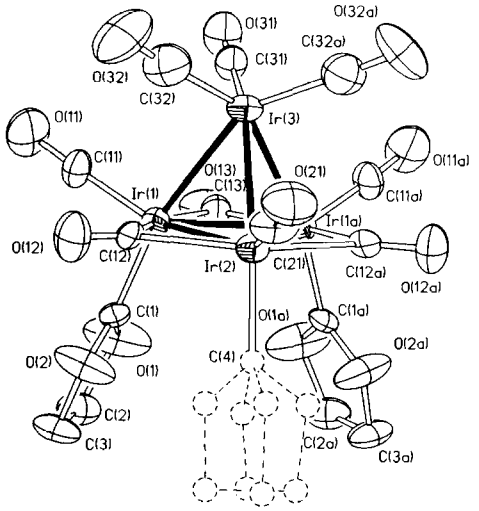

Fig. 7. ORTEP plot (50% of probability) of $[Ir_4(CO)_9(\overline{COCH_2CH_2O})_3]$ (**4**) with atom labelling scheme.

are 32, 27 and 21°, respectively, and are significantly greater than in **2**. All Ir–Ir distances are also significantly longer than in **2**. The Ir–CO distances for terminal COs (mean 1.89(5) Å) are shorter than for bridging COs (mean 2.10(4) Å).

Molecular structure of $[Ir_4(CO)_9(\overline{COCH_2CH_2O})_3]$ (4)

Figure 7 shows a perspective view of the molecule. The cluster lies on a crystallographic mirror plane passing through Ir(2), Ir(3), CO(31), CO(13), CO(21) and has a disordered carbenic ligand. Three edges of a triangular face of the Ir_4 tetrahedron are symmetrically bridged by three carbonyls, and are shorter (mean Ir–Ir 2.718(2) Å) than the unbridged Ir–Ir bonds (mean Ir–Ir

TABLE 4. Selected bond distances (Å) and angles (°) in **2**, **3** and **4** with standard deviations in parentheses

$[Ir_4(CO)_{11}(\overline{COCH_2CH_2O})]$			
Ir(1)–Ir(2)	2.694(1)	Ir(3)–C(1)	1.94(3)
Ir(1)–Ir(3)	2.674(1)	C(1)–O(1)	1.29(4)
Ir(1)–Ir(4)	2.687(1)	C(1)–O(2)	1.39(4)
Ir(2)–Ir(3)	2.679(1)	C(2)–O(2)	1.44(5)
Ir(2)–Ir(4)	2.688(1)	C(2)–C(3)	1.49(6)
Ir(3)–Ir(4)	2.672(1)	C(3)–O(1)	1.40(5)
Ir–CO(mean)	1.88(3)	C–O(mean)	1.14(4)
Ir–Ir–Ir(mean)	60.0(1)	Ir–C–O(mean)	175(3)
Ir(3)–C(1)–O(1)	129.9(20)	C(21)–Ir(2)–C(22)	103.1(13)
Ir(3)–C(1)–O(2)	121.9(21)	C(21)–Ir(2)–C(23)	101.3(12)
C(1)–O(1)–C(3)	113.6(28)	C(22)–Ir(2)–C(23)	100.8(1)
O(1)–C(1)–O(2)	105.7(27)	C(1)–Ir(3)–C(31)	92.4(15)
C(1)–O(2)–C(2)	112.2(26)	C(1)–Ir(3)–C(32)	100.2(13)
O(2)–C(2)–C(3)	99.6(29)	C(31)–Ir(3)–C(32)	101.6(16)
C(2)–C(3)–O(1)	106.3(35)	C(41)–Ir(4)–C(42)	94.0(13)
C(11)–Ir(1)–C(13)	99.8(11)	C(41)–Ir(4)–C(43)	103.7(12)
C(11)–Ir(1)–C(12)	97.5(11)	C(42)–Ir(4)–C(43)	103.8(11)
C(12)–Ir(1)–C(13)	102.8(11)		
$[Ir_4(CO)_{10}(\overline{COCH_2CH_2O})_2]$			
Ir(1)–Ir(2)	2.728(4)	C(1)–O(2)	1.27(8)
Ir(1)–Ir(3)	2.733(3)	C(2)–C(3)	1.42(8)
Ir(1)–Ir(4)	2.738(4)	C(2)–O(1)	1.53(6)
Ir(2)–Ir(3)	2.732(4)	C(3)–O(2)	1.57(7)
Ir(2)–Ir(4)	2.754(4)	Ir–CO_{unbr}(mean)	1.89(5)
Ir(3)–Ir(4)	2.723(4)	Ir–CO_{br}(mean)	2.10(4)
Ir(1)–C(4)	1.96(5)	C–O_{unbr}(mean)	1.15(6)
Ir(2)–C(1)	2.06(6)	C–O_{br}(mean)	1.17(5)
C(1)–O(1)	1.27(8)		
Ir–Ir–Ir(mean)	60.0(1)	C(1)–Ir(2)–C(21)	92.8(22)
Ir–C–O_{unbr}(mean)	173(4)	C(12)–Ir(2)–C(21)	96.0(19)
Ir–C–O_{br}(mean)	138(3)	C(23)–Ir(2)–C(21)	99.1(15)
C(4)–Ir(1)–C(11)	97.5(20)	C(13)–Ir(3)–C(23)	154.6(15)
C(4)–Ir(1)–C(12)	96.2(20)	C(13)–Ir(3)–C(31)	96.8(19)
C(11)–Ir(1)–C(12)	98.7(21)	C(23)–Ir(3)–C(31)	92.9(18)
C(4)–Ir(1)–C(13)	95.9(19)	C(13)–Ir(3)–C(32)	97.9(21)
C(11)–Ir(1)–C(13)	98.2(20)	C(23)–Ir(3)–C(32)	103.3(20)
C(12)–Ir(1)–C(13)	157.8(16)	C(31)–Ir(3)–C(32)	100.5(24)
C(1)–Ir(2)–C(12)	93.7(20)	C(41)–Ir(4)–C(42)	97.9(20)
C(1)–Ir(2)–C(23)	93.7(19)	C(41)–Ir(4)–C(43)	105.3(18)
C(12)–Ir(2)–C(23)	162.8(18)	C(42)–Ir(4)–C(43)	108.6(22)
$[Ir_4(CO)_9(\overline{COCH_2CH_2O})_3]$ (label 'a' refers to atoms related by the crystallographic mirror plane)			
Ir(1)–Ir(2)	2.725(1)	C(1)–O(2)	1.30(3)
Ir(1)–Ir(3)	2.735(2)	C(2)–C(3)	1.43(4)
Ir(1)–Ir(1a)	2.712(2)	C(2)–O(1)	1.56(4)
Ir(2)–Ir(3)	2.744(2)	C(3)–O(2)	1.49(3)
Ir(2)–Ir(1a)	2.725(1)	Ir–CO_{unbr}(mean)	1.86(3)
Ir(3)–Ir(1a)	2.735(2)	Ir–CO_{br}(mean)	2.09(3)
Ir(1)–C(1)	1.96(2)	C–O_{unbr}(mean)	1.16(4)
Ir(2)–C(4)	1.96(4)	C–O_{br}(mean)	1.20(4)
C(1)–O(1)	1.32(3)		
Ir–Ir–Ir(mean)	59.9(1)	C(12)–Ir(2)–C(21)	99.0(5)
Ir–C–O_{unbr}(mean)	176(3)	C(12)–Ir(2)–C(4)	95.5(5)
Ir–C–O_{br}(mean)	139(1)	C(21)–Ir(2)–C(4)	94.0(13)
C(11)–Ir(1)–C(12)	98.7(10)	C(12)–Ir(2)–C(12a)	158.1(10)
C(11)–Ir(1)–C(13)	99.0(11)	C(21)–Ir(2)–C(12a)	99.0(5)
C(12)–Ir(1)–C(13)	158.8(8)	C(4)–Ir(2)–C(12a)	95.5(5)
C(11)–Ir(1)–C(1)	96.3(10)	C(31)–Ir(3)–C(32)	104.6(13)
C(12)–Ir(1)–C(1)	94.8(8)	C(31)–Ir(3)–C(32a)	104.6(13)
C(13)–Ir(1)–C(1)	94.7(11)	C(32)–Ir(3)–C(32a)	108.4(20)

2.739(2) Å) with a trend opposite to the most common behaviour [15]. The Ir–Ir bonds are longer than in the monosubstituted derivative. The three carbenic ligands are axial with respect to the plane containing the bridging COs; the Ir(1)–C(1) and Ir(2)–C(4) bonds form angles of 70 and 72°, respectively, with the Ir(1)–Ir(1a)–Ir(2) plane; the terminal CO(11) and CO(12) have tilting angles of 27 and 22°, respectively, with respect to the previous plane. The mean deviation of the bridging COs from the plane Ir(1)–Ir(1a)–Ir(2) is 0.03 Å.

Relevant bond distances and angles are given in Table 4 for the three complexes. Comparing the three derivatives, the prevalent influence of bridging CO groups with respect to the carbenic ligands in determining geometry is evident: the presence of bridging COs on the basal plane push the terminal radial COs towards the fourth iridium atom and the axial ligands follow this movement moving towards the basal plane. The carbenic ligands are more or less puckered: the non-disordered rings show a mean deviation from planarity of 0.06 Å in **2** and **3** and of 0.02 Å in **4**. No intermolecular contacts occur in the three complexes.

Supplementary material

Complete list of structural parameters and lists of structure factors are available from G.G. upon request.

Acknowledgements

We thank the Swiss National Science Foundation for financial support, Dr Orrell for a copy of the D2DNMR program and Dr G. Suardi for a preliminary study of **3**.

References

1 M.M. Singh and R.J. Angelici, *Angew. Chem., Int. Ed. Engl., 22* (1983) 163; *Inorg. Chem., 23* (1984) 2691, 2699; *Inorg. Chim. Acta, 100* (1985) 57.
2 S. Jy Wang, L.L. Miller, R.A. Jacobson and R.J. Angelici, *Inorg. Chim. Acta, 145* (1988) 129.
3 P. Chini, G. Ciani, L. Garlaschelli, M. Manassero, S. Martinengo and A. Sironi, *J. Organomet. Chem., 152* (1978) C35; L. Garlaschelli, S. Martinengo and P. Chini, *J. Organomet. Chem., 213* (1981) 379.
4 R. Ros, A. Scrivanti, V.G. Albano, D. Braga and L. Garlaschelli, *J. Chem. Soc., Dalton Trans.,* (1986) 2411.
5 A. Strawczynski, G. Suardi, R. Ros and R. Roulet, *Helv. Chim. Acta, 76* (1993) in press.
6 A. Orlandi, R. Ros and R. Roulet, *Helv. Chim. Acta, 74* (1991) 1464.
7 *EXCHANGE,* Program Library, Computing Center, University of Lausanne.
8 A. Strawczynski, R. Ros and R. Roulet, *Helv. Chim. Acta, 71* (1988) 867.
9 G.F. Stuntz and J.R. Shapley, *Inorg. Chem., 15* (1976) 1994; *J. Am. Chem. Soc., 99* (1977) 607; K.J. Karel and J.R. Norton, *J. Am. Chem. Soc., 96* (1974) 6812.
10 B.E. Mann, C.M. Spencer and A.K. Smith, *J. Organomet. Chem., 244* (1983) C17; B.E. Mann, B.T. Pickup and A.K. Smith, *J. Chem. Soc., Dalton Trans.,* (1989) 889; B.E. Mann, M.D. Vargas and R. Khadar, *J. Chem. Soc., Dalton Trans.,* (1992) 1725.
11 G.F. Stuntz and J.R. Shapley, *J. Organomet. Chem., 213* (1981) 389.
12 A. Orlandi, U. Frey, G. Suardi, A.E. Merbach and R. Roulet, *Inorg. Chem., 31* (1992) 1304.
13 J.R. Shapley, G.F. Stuntz, M.R. Churchill and J.P. Hutchinson, *J. Chem. Soc., Chem. Commun.,* (1979) 219.
14 M.R. Churchill and J.P. Hutchinson, *Inorg. Chem., 9* (1979) 2451.
15 D. Braga and F. Grepioni, *J. Organomet. Chem., 336* (1987) C9.